Comparison BIPM.RI(I)-K6 of the standards for absorbed dose to water of the KRISS, Korea and the BIPM in accelerator photon beams

C. Kessler [1], D.T. Burns [1], S. Picard[1], P. Roger[1], I.J. Kim [2], B.C. Kim [2], Y.H. Kim [2], J.H. Kim [2], J.P. Chung [2], C.Y. Yi [2]

[1] Bureau International des Poids et Mesures, F-92310 Sèvres Cedex
[2] Korea Research Institute of Standards and Science, Daejeon 34113, Korea

Abstract

A key comparison has been made between the absorbed dose to water standards of the KRISS, Korea and the BIPM in accelerator photon beams. The results show the standards to be in agreement within the expanded uncertainty ($k = 2$) of the comparison of 12 parts in 10^3. The results are analysed and presented in terms of degrees of equivalence, suitable for entry in the BIPM key comparison database.

1. Introduction

An indirect comparison has been made between the absorbed dose to water standards of the Korea Research Institute of Standards and Science (KRISS), Korea, and the Bureau International des Poids et Mesures (BIPM) in accelerator photon beams ranging from 6 MV to 18 MV. The comparison took place using the BIPM accelerator facility at the DOSEO platform in Saclay (France) in November 2017. The comparison was undertaken using two transfer ionization chambers type PTW 30013 belonging to the KRISS. The results of the comparison are given in terms of the mean ratio of the calibration coefficients of these transfer instruments determined at the two laboratories for three radiation qualities. The final results were supplied by the KRISS in July 2018.

2. Details of the standards

BIPM primary standard

The BIPM primary standard is a graphite calorimeter described by Picard *et al.* (2009). The calorimeter consists of a graphite core placed in a cylindrical graphite jacket; the main characteristics are listed in Table 1. The core is equipped with three thermistor pairs connected to three independent d.c. bridges. This core and jacket are placed in an evacuated cubic PMMA vacuum phantom with side length 300 mm. A graphite build-up plate is used to position the calorimeter centre at the reference depth of 10 g cm^{-2}. Two nominally-identical parallel-plate ionization chamber standards with graphite walls and collector, similar in design to the existing BIPM standards for air kerma and absorbed dose to water, were fabricated to serve in the determination of the absorbed dose to water from the measured absorbed dose to the graphite core. The first chamber is housed in a graphite jacket, nominally identical to the calorimeter jacket, and is positioned in the same PMMA vacuum phantom but at ambient air pressure, replacing the calorimeter core and its jacket. The second chamber is housed in a waterproof polyethylene sleeve and mounted at a depth of 10 g cm^{-2} in a PMMA water

phantom with the same outer dimensions and PMMA window thickness (4 mm) as the vacuum phantom.

Table 1. Characteristics of the BIPM standard

BIPM standard		Dimensions
Calorimeter core	Diameter / mm	45.0
	Thickness / mm	6.7
Calorimeter jacket	Diameter / mm	60.0
	Thickness / mm	32.0
Chamber	Diameter / mm	45.0
	Thickness / mm	11.0
Air cavity	Volume / cm^3	6.8
Wall	Thickness / mm	2.85
	Material	Graphite
	Density / g cm^{-3}	1.85
Voltage applied to outer electrode / V	Positive polarity	80

KRISS Primary standard

The primary standard of the KRISS is a graphite calorimeter described by Kim *et al.* (2017). The calorimeter consists of a graphite core surrounded by two layers of graphite jackets, and operates in the quasi-adiabatic mode (Seuntjens and DuSautoy 2003). To achieve quasi-adiabatic conditions, the temperature of the inner-jacket is controlled by a thermal feedback circuit so that temperature difference from the core can be kept constant. The core and the jackets are evacuated for better temperature control. The vacuum housing is similar to that of the graphite calorimeter GR9 of the French national laboratory (Ostrowsky and Daures 2008). The calorimeter is placed in a graphite phantom with dimensions 30x30x18 cm^3. The core is placed at the source-axis distance (SAD) of 100 cm and at the depth of 10 g cm^{-2}.
The core is equipped with three thermistor sensors and one thermistor heater. The three thermistor sensors are connected in series to a d.c. bridge to detect the average temperature rise of the core. The thermistor heater is connected to a power source in series with a precision resistor (10 kΩ) and the potential drops across the heater and the precision resistor are measured to determine the electrical energy dissipated in the core. The main characteristics of the core are listed in Table 2.

Table 2. Characteristics of the KRISS standard

KRISS standard		Dimensions
Calorimeter core	Diameter / mm	16
	Thickness / mm	3
Calorimeter inner jacket	Diameter / mm	26
Calorimeter outer jacket	Diameter / mm	40

KRISS uses a set of two thimble-type ionization chambers (Exradin A2, 0.53 cm^3) connected in parallel to a Keithley electrometer 6517B to serve as a monitor during irradiation. The

monitor chambers are placed at 66 cm from the target and separated from each other by 12.5 cm in the cross-plane of the accelerator.

3. Determination of the absorbed dose to water

3.1 Absorbed dose to water at the BIPM

At the BIPM the absorbed dose to water rate is determined from calorimetric and ionometric measurements combined with Monte Carlo calculations. The method is described in Burns (2019) and in a number of previous comparison reports, for example Picard *et al.* (2016). The absorbed dose to water at the reference depth, $D_{\mathrm{w,BIPM}}$, is evaluated as

$$D_{\mathrm{w,BIPM}} = D_{\mathrm{c}} \frac{Q_{\mathrm{w}}}{Q_{\mathrm{c}}} \left(\frac{D_{\mathrm{w}}}{D_{\mathrm{c}}}\right)^{\mathrm{MC}} \left(\frac{D_{\mathrm{cav,c}}}{D_{\mathrm{cav,w}}}\right)^{\mathrm{MC}} k_{\mathrm{rn}} \qquad (1)$$

where

D_{c}	measured absorbed dose to the graphite core;
Q_{c}	ionization charge measured by the standard chamber positioned in the graphite jacket, replacing the core;
Q_{w}	ionization charge measured by the standard chamber positioned in water;
$(D_{\mathrm{w}}/D_{\mathrm{c}})^{\mathrm{MC}}$	calculated ratio of absorbed dose to water and to the graphite core using Monte Carlo simulations;
$\left(D_{\mathrm{cav,c}}/D_{\mathrm{cav,w}}\right)^{\mathrm{MC}}$	calculated ratio of cavity doses in graphite and in water using Monte Carlo simulations;
k_{rn}	measured correction for radial non-uniformity in water.

The ionization charges Q_{w} and Q_{c} are normalized to 293.15 K and 101.325 kPa and corrected for ion recombination, as explained at the end of this section. Although the two standard chambers are nominally identical, the air cavity volume for each is known and a correction k_{vol} is made for the small difference in volume with a relative standard uncertainty of 3 parts in 10^4.

Equation 1 can also be expressed as

$$\begin{aligned} D_{\mathrm{w,BIPM}} &= Q_{\mathrm{w}} \frac{D_{\mathrm{c}}}{Q_{\mathrm{c}}} C_{\mathrm{w,c}} k_{\mathrm{rn}} \\ &= Q_{\mathrm{w}} N_{D\mathrm{c}} C_{\mathrm{w,c}} k_{\mathrm{rn}} \end{aligned} \qquad (2)$$

where

$C_{\mathrm{w,c}}$ represents the total Monte Carlo conversion factor and

$N_{D\mathrm{c}}$ is the measured calibration coefficient for the standard chamber in graphite

- *Monte Carlo conversion factor $C_{\mathrm{w,c}}$*

During the period 2009-2015, twenty calculations of the conversion factor $C_{\mathrm{w,c}}$ were made using the sets of phase-space files provided by the National Measurement Institutes (NMIs) that participated in the BIPM.RI(I)-K6 key comparison. Figure 1 shows the conversion factors plotted as a function of the calculated $\mathrm{TPR}_{20,10}$; a quadratic fit to these data, weighted with the statistical uncertainty of each point, shows the deviations to be consistent with the typical

statistical standard uncertainty of 5 parts in 10^4. For the present comparison, the dose conversion factors presented in Table 3 are obtained using the quadratic fit and the $TPR_{20,10}$ values measured at the BIPM facility. A type A uncertainty of 5 parts in 10^4 arising from the fitting procedure is included in Table 12, as well as the type B uncertainty for $C_{w,c}$ of 2.5 parts in 10^3 derived from Burns (2019).

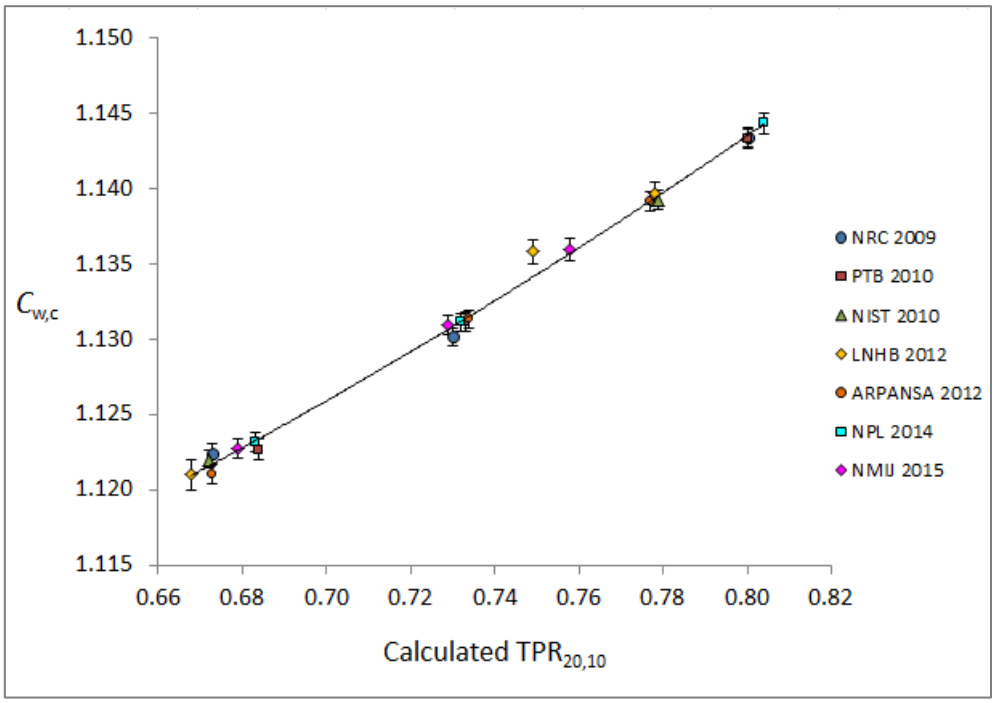

Figure 1. The dose conversion factor $C_{w,c}$ for the BIPM standard, calculated using the phase-space files supplied by participating NMIs. The line is a weighted quadratic fit to the data; the deviations about this line are consistent with the typical statistical standard uncertainty of 5 parts in 10^4.

- *Calibration coefficient* N_{Dc}

During each comparison, the calibration coefficient N_{D_c} for the standard chamber in graphite has been measured and plotted as a function of the measured $TPR_{20,10}$. Figure 2 shows the normalized N_{D_c} determinations and a quadratic fit to the data; the plot also shows the coefficients determined at the BIPM facility, which are included in the fit.

For the present comparison, the calibration coefficients N_{Dc} for the standard chamber in graphite for the BIPM $TPR_{20,10}$ values are taken to be those derived from the quadratic fit and are presented in Table 3. The uncertainty arising from the fitting procedure is taken as the r.m.s. deviation of the measured values from the fitted curve (2.3 parts in 10^3) and is included in Table 12. By its nature, this includes the statistical uncertainties associated with the BIPM calorimeter and well as those arising from differences in spectra at the NMI accelerators.

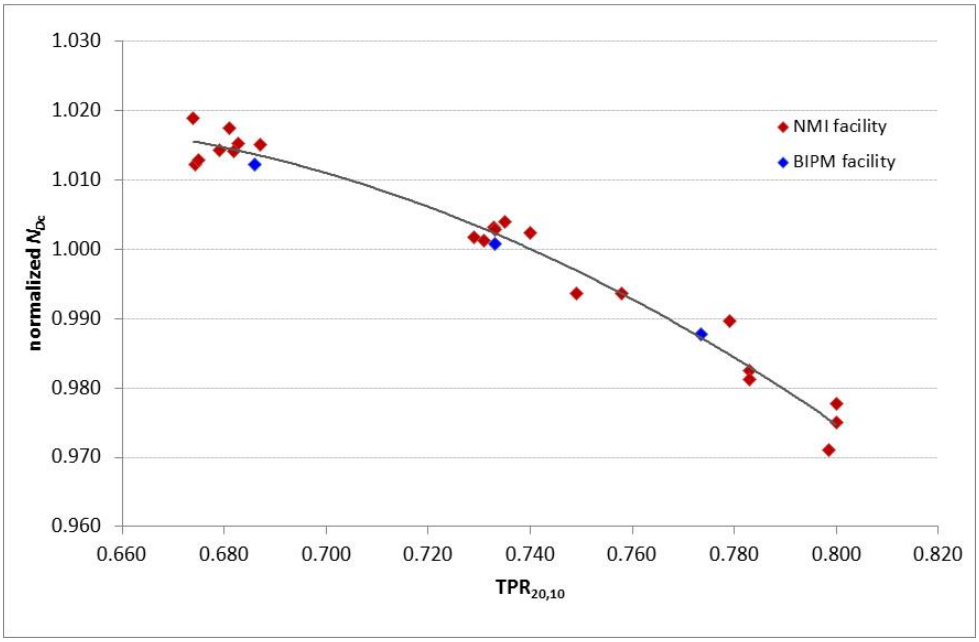

Figure 2. The calibration coefficients N_{Dc}, normalized to the mean, as a function of the measured $TPR_{20,10}$. The solid line is a quadratic fit to the combined data set.

Table 3. Conversion factor and calibration coefficient

Radiation quality	6 MV	10 MV	18 MV
$TPR_{20,10}$	0.686	0.733	0.774
$C_{w,c}$ (fit)	1.1229	1.1306	1.1377
N_{Dc} (fit)	4.011	3.966	3.906

As mentioned above, the ionization charges Q_w and Q_c are normalized to 293.15 K and 101.325 kPa; no correction for humidity is applied. The temperature is measured using a calibrated thermistor, placed inside the waterproof envelope and inside the graphite jacket for measurements in water and graphite, respectively.

The ionization charges Q_w and Q_c are corrected for ion recombination. The correction factor k_s for losses due to ion recombination for the standard chambers in graphite and water were determined using the method of Niatel as described by Boutillon (1998) for continuous radiation and by Picard *et al.* (2011) for pulsed radiation.

The recombination correction k_s for pulsed radiation can be expressed as

$$k_s = 1 + k_{\text{init}} + k_{\text{vol}} Q_p \qquad (3)$$

where Q_p is the charge per pulse expressed in pC. Table 4 gives the values for k_{init} and k_{vol}.

Table 4. Ion recombination for the BIPM standard chambers

BIPM Standard	Water standard [a]	Graphite standard [a]
initial recombination and diffusion, k_{init}	16.4×10^{-4}	18.8×10^{-4}
volume recombination coefficient, k_{vol} / pC^{-1}	1.43×10^{-4}	1.13×10^{-4}

[a] The standards in water and graphite are identified as CALO5 and CALO6c, respectively

For a typical charge per pulse of up to 100 pC, k_s is of the order of 1 part in 10^2 and the standard uncertainty for k_s is estimated to be 5 parts in 10^4, included in Table 12.

The factors that correct for the non-uniformity of the beams were calculated from the measured beam profiles in water. For graphite, it is assumed that the correction cancels as the standard chamber in graphite has the same dimensions as the calorimeter core. The correction factors are listed in Table 5. A relative standard uncertainty of 1 part in 10^3 is introduced for this effect in Table 12.

Table 5. Radial non-uniformity correction in water

Radiation quality	6 MV	10 MV	18 MV
radial non-uniformity k_{rn}	0.9995	0.9928	1.0000

3.2 Absorbed dose to water at the KRISS

The average absorbed dose rate to the graphite core, $\overline{D}_{\mathrm{C,KRISS}}/Q_{\mathrm{mon}}$, can be expressed as follows

$$\left(\frac{\overline{D}_{\mathrm{C,KRISS}}}{Q_{\mathrm{mon}}}\right) = \frac{C_{\mathrm{C,eff}}}{m_{\mathrm{eff,KRISS}}}\left(\frac{\Delta T_{\mathrm{irr}}}{Q_{\mathrm{mon}}}\right) \quad (4)$$

where

$C_{\mathrm{C,eff}}$ is the effective heat capacity

$m_{\mathrm{eff,KRISS}}$ is the effective mass of the core

ΔT_{irr} is the temperature rise of the core

Q_{mon} is the ionization charge (after correction for temperature and pressure) of the monitor chamber

The effective heat capacity $C_{\mathrm{C,eff}}$ is determined from the temperature rise of the core ΔT_{cal} which is induced by a known amount of electrical energy E_{cal} dissipated in the core by the thermistor heater:

$$C_{\mathrm{C,eff}} = \frac{\Delta T_{\mathrm{cal}}}{E_{\mathrm{cal}}} \quad (5)$$

The effective mass of the core $m_{\mathrm{eff,KRISS}}$ is determined as:

$$m_{\mathrm{eff,KRISS}} = m_{\mathrm{C,KRISS}} + \sum_{i=1}^{n} m_i \left(\frac{\overline{D}_i}{\overline{D}_{\mathrm{C}}}\right) \quad (6)$$

where

$m_{\mathrm{C,KRISS}}$ is the mass of graphite

m_i represents the impurities of the core

$\overline{D}_{\mathrm{C}}$, $\overline{D}_i$ represent average absorbed dose in the graphite and in the impurities of the core, respectively.

Under the assumption of charge-particle equilibrium, the ratio of $(\overline{D}_{\mathrm{C}}/\overline{D}_i)$ is estimated by the product of photon energy fluence and the mean mass energy-absorption coefficients. The mass energy-absorption coefficient is obtained using the subroutine 'mutren' of PENELOPE code (Salvat *et al*. 2011) and the photon energy fluence is calculated using the EGSnrc code (Kawrakow *et al*. 2015).

The absorbed dose rate to water at the reference depth, $D_{\mathrm{W,KRISS}}/Q_{\mathrm{mon}}$, is determined from the absorbed dose rate to the graphite core, $\overline{D}_{\mathrm{C,KRISS}}/Q_{\mathrm{mon}}$, as

$$\left(\frac{D_{\mathrm{W,KRISS}}}{Q_{\mathrm{mon}}}\right) = \left(\frac{\bar{D}_{\mathrm{C,KRISS}}}{Q_{\mathrm{mon}}}\right)\left(\frac{\bar{D}_{\mathrm{W}}}{\bar{D}_{\mathrm{C}}}\right) k_{\mathrm{w,rn,KRISS}} \frac{1}{k_{\mathrm{BS}}} \qquad (7)$$

where

$\left(\frac{\bar{D}_{\mathrm{W}}}{\bar{D}_{\mathrm{C}}}\right)$ is the conversion factor of absorbed dose to graphite to absorbed dose to water, calculated using the EGSnrc Monte Carlo code

$k_{\mathrm{w,rn,KRISS}}$ is the correction factor for radial non-uniformity in water of the KRISS beam over the cross section of the graphite core

k_{BS} represents correction for difference of backscattering from different phantoms of graphite and water to the monitor chamber

The calculated conversion factors $\left(\frac{\bar{D}_{\mathrm{W}}}{\bar{D}_{\mathrm{C}}}\right)$ are plotted as a function of the $\mathrm{TPR}_{20,10}$ in Figure 3.

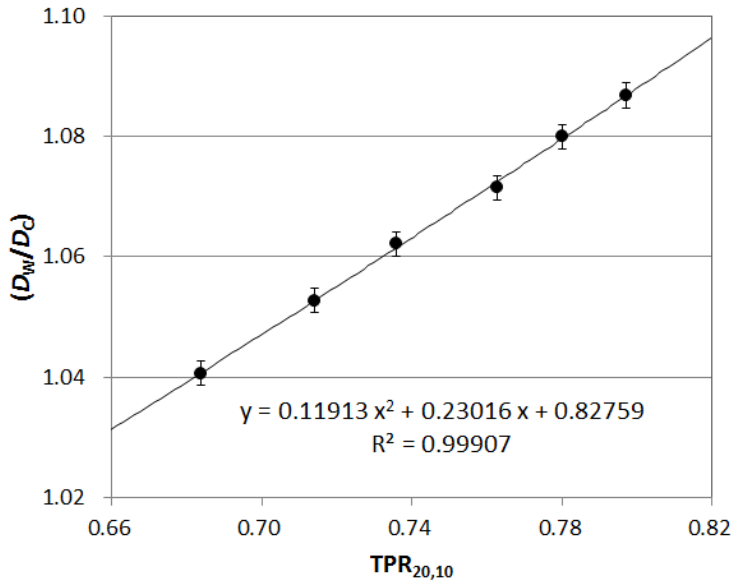

Figure 3. The conversion factor of absorbed dose to graphite to absorbed dose to water for the KRISS calorimeter. The solid line represents the quadratic fit to the data points. Uncertainty bars represent the standard uncertainty.

Transfer chambers are positioned in a water phantom of 30×30×30 cm^3 at the source to chamber distance (SCD) of 100 cm and at the reference depth of water (10 g cm^{-2}). The absorbed dose calibration coefficient, $N_{\mathrm{D,w,KRISS}}$, of a transfer chamber is determined as

$$N_{D_{\mathrm{W}},\mathrm{KRISS}} = \left(\frac{D_{\mathrm{W,KRISS}}}{Q_{\mathrm{mon}}}\right)\left(\frac{Q_{\mathrm{mon}}}{Q_{\mathrm{W,KRISS}}}\right)\frac{1}{k_{\mathrm{elec}}k_{\mathrm{TP}}k_{\mathrm{s}}k_{\mathrm{Q,rn}}} \qquad (8)$$

where

$Q_{\mathrm{W,KRISS}}$ is the ionization charge measured using the transfer chamber in water

k_{elec} is the calibration coefficient of the electrometer.

k_{TP} is the pressure and temperature correction

k_{s} is the ion recombination correction

k_{Qrn} is the correction for the radial non-uniformity of the KRISS beam across the cavity of the transfer chamber

4. BIPM irradiation facility

The BIPM irradiation facility and reference beam qualities

The comparison was carried out at the DOSEO platform in Saclay (France), which houses an Elekta *Versa* linear clinical accelerator. This accelerator provides three high-energy photon beams at 6 MV, 10 MV and 18 MV. The radiation qualities are characterized in terms of the tissue-phantom ratio $TPR_{20,10}$, the measured values given in Table 3.

All measurements were made with the gantry fixed for horizontal irradiation, with a source-detector distance of 1 m and at the reference depth of 10 g cm^{-2}.

The irradiation area is temperature controlled at 20 °C. The relative humidity is controlled within the range from 40 % to 50 %. Air temperature, pressure and humidity are measured using a commercial instrument. The water temperature is measured using a calibrated thermistor.

The beam output is monitored during irradiation using a commercial parallel-plate transmission chamber fixed to a shadow tray; the day-to-day stability of the transmission chamber is determined by comparing its response to a thimble chamber type NE 2571. This monitoring system is described in previous comparison reports, for example Picard *et al.* (2016).

5. Comparison procedure

The comparison of the KRISS and BIPM standards was made indirectly using the calibration coefficients $N_{D_w,\mathrm{lab}}$ for two transfer chambers given by

$$N_{D_\mathrm{w},\mathrm{lab}} = \dot{D}_{\mathrm{w,lab}} \big/ I_{\mathrm{lab}} \,, \qquad (9)$$

where $\dot{D}_{\mathrm{w,lab}}$ is the water absorbed dose rate at the KRISS or the BIPM and I_{lab} is the corresponding ionization current for a transfer chamber measured at each laboratory.
The ionization chambers PTW 30013, serial numbers 8979 and 9304, belonging to the KRISS, are the transfer chambers used for this comparison. Their main characteristics are listed in Table 6.

Table 6. Characteristics of the transfer chambers type PTW 30013

Design cylindrical, water-proof - Nominal values		8979	9304
Dimensions of sensitive volume	radius / mm	3.05	
	length / mm	25.9	
Volume	air cavity / cm^3	0.6	
Wall	material, density	0.335 mm PMMA, 1.19 g cm^{-3} 0.09 mm graphite, 1.85 g cm^{-3}	
Applied voltage to outer electrode	negative polarity / V	250	400

These chambers were calibrated at the KRISS before and after the measurements at the BIPM. The essential details for the determination of the calibration coefficients N_{D_w} for the transfer chambers are described below.

Positioning
At each laboratory the chambers were positioned with the stem perpendicular to the beam direction and with the appropriate marking on the stem and waterproof sleeve facing the source.

Applied voltage and polarity

A collecting voltage of 250 V and 400 V (negative polarity) was applied to the outer electrode of the chambers sn 8979 and sn 9304, respectively, at least 30 min before any measurements were made. No corrections were applied at either laboratory for polarity.

Ion recombination

Ion recombination was measured for a PTW 30013 belonging to the BIPM for the two polarizing voltages used at the KRISS using the Niatel method as implemented for pulsed beams in Picard *et al.* (2011) using equation 3. The results are presented in Table 7. For the 18 MV radiation quality, the correction factor k_s was also determined using the two voltage technique, as described in the code of practice TRS-398 (IAEA 2000). The results are included in the table.

Table 7. Ion recombination for the PTW 30013 determined at the BIPM

Voltage	k_{init}	k_{vol} / pC^{-1}	k_s			
			6 MV	10 MV	18 MV	TRS-398
250 V	13.6×10^{-4}	6.6×10^{-4}	1.0039	1.0057	1.0073	1.0072
400 V	8.6×10^{-4}	4.1×10^{-4}	1.0024	1.0035	1.0045	1.0039

At the KRISS, the correction for ion recombination was determined for the transfer chambers using the method described in Burns and McEwen (1998). The corrections applied at the KRISS are listed in Table 8.

Re-evaluating this correction for the charge per pulse measured at the KRISS but using the BIPM determination of the recombination coefficients, the ion recombination correction for each chambers differs by no more than 5 parts in 10^4, in agreement with the KRISS values within the uncertainties.

Table 8. Ion recombination for the PTW 30013 applied at the KRISS

Voltage	k_{init}	k_{vol} / pC^{-1}	k_s		
			6 MV	10 MV	18 MV
250 V	6.8×10^{-4}	7.0×10^{-4}	1.0034	1.0048	1.0043
400 V	6.1×10^{-4}	4.1×10^{-4}	1.0021	1.0029	1.0026

Radial non-uniformity correction

The correction for the radial non-uniformity of the beam over the section of the transfer chambers is estimated to be 0.9980 for the 10 MV quality and unity for the other two qualities, with an uncertainty of 5×10^{-4}. At the KRISS, the correction applied is 0.9995 for 6 MV, 0.9980 for 10 MV and 0.9975 for 18 MV, with an uncertainty of 1×10^{-3}.

Charge measurements

The charge Q was measured at the BIPM using a Keithley electrometer, model K6517B and a set of calibrated external capacitors. The chambers were pre-irradiated each day for at least 10 min ($\approx$ 20 Gy) at the BIPM, and for at least 3 min ($\approx$ 5 Gy) at the KRISS before any measurements were made.

Ambient conditions

At the BIPM, the water temperature is measured for each current measurement and it was stable to better than 0.1 °C. At the KRISS, the water temperature was stable to within 0.2 °C. The ionization current is normalized to 293.15 K and 101.325 kPa at both laboratories.
Relative humidity is in the range from 40 % to 50 % at the BIPM and from 30 % to 70 % at the KRISS. Consequently, no correction for humidity is applied to the ionization current measured.

PMMA phantom window and sleeve

Both laboratories use a horizontal radiation beam and the thickness of the PMMA front window of the water phantom is included as a water-equivalent thickness in g cm^{-2} when positioning the chamber.
A PMMA waterproof sleeve 0.8 mm in thickness was supplied by the KRISS for the PTW chambers. The same sleeve was used at both laboratories and, consequently, no correction for the influence of each sleeve was necessary at either laboratory.

6. Results of the comparison

Each PTW 30013 transfer chamber was positioned and measured in the BIPM beams on four separate occasions. The results were reproducible to better than 1×10^{-3}. At the KRISS, the chambers were calibrated by direct comparison with the calorimeter three times before and once after the measurements at the BIPM. The KRISS results are presented in Table 9. The values $N_{D\mathrm{w,KRISS}}$ measured before and after the measurements at the BIPM give rise to the relative standard uncertainties $s_{\mathrm{st},1}$ and $s_{\mathrm{st},2}$ for the two chambers, which are taken to represent the uncertainty in $N_{D\mathrm{w}}$ associated with transfer chamber stability. The mean value of s_{st} for the three qualities, $s_{\mathrm{st}} = 0.0005$, is a global representation of the comparison uncertainty arising from the transfer chambers and is included in Table 16.

Table 9. Calibration coefficients for the transfer chambers at the KRISS

Radiation quality	6 MV	10 MV	18 MV
$TPR_{20,10}$	0.684	0.734	0.778
PTW 30013-8979			
$N_{D_{\mathrm{w}},\mathrm{KRISS}}$ / Gy μC^{-1} (pre-BIPM)	53.03	52.59	52.02
$N_{D_{\mathrm{w}},\mathrm{KRISS}}$ / Gy μC^{-1} (post-BIPM)	53.01	52.57	52.13
$s_{\mathrm{st},1}$ (relative)	0.0002	0.0002	0.0011
PTW 30013-9304			
$N_{D_{\mathrm{w}},\mathrm{KRISS}}$ / Gy μC^{-1} (pre-BIPM)	53.28	52.84	52.28
$N_{D_{\mathrm{w}},\mathrm{KRISS}}$ / Gy μC^{-1} (post-BIPM)	53.24	52.82	52.39
$s_{\mathrm{st},2}$ (relative)	0.0004	0.0002	0.0011

As can be seen from Tables 3 and 9, there is no significant difference in the $TPR_{20,10}$ values for the two laboratories. For each chamber, a quadratic fit was made to the mean of the KRISS results before and after the BIPM measurements to interpolate the calibration coefficients for the BIPM $TPR_{20,10}$.

The result of the comparison, R_{D_w} , is expressed in the form

$$R_{D_w} = N_{D_w,\mathrm{KRISS}} \big/ N_{D_w,\mathrm{BIPM}} \,, \qquad (10)$$

The final KRISS results $N_{D_w,\mathrm{KRISS}}$ for each chamber calculated for the BIPM beams and the BIPM results $N_{D_w,\mathrm{BIPM}}$ are presented in Table 10.

Table 10. Calibration coefficients for the transfer chambers

Radiation quality	6 MV	10 MV	18 MV
PTW 30013-8979			
$N_{D_w,\mathrm{KRISS}}$ / Gy μC^{-1} (interpolated)	53.01	52.59	52.13
$N_{D_w,\mathrm{BIPM}}$ / Gy μC^{-1}	52.58	52.30	51.69
PTW 30013-9304			
$N_{D_w,\mathrm{KRISS}}$ / Gy μC^{-1} (interpolated)	53.25	52.84	52.39
$N_{D_w,\mathrm{BIPM}}$ / Gy μC^{-1}	52.84	52.54	51.95

The final comparison results $R_{D\mathrm{w,KRISS}}$ given in Table 11 are evaluated as the mean for the two transfer chambers. For each beam quality, the corresponding uncertainty is the standard uncertainty of this mean. The mean value for the three qualities, $s_{\mathrm{tr},}$ = 0.0001, represents the comparison uncertainty arising from the difference in the results for the two transfer chambers and is included in Table 16.

Table 11. Comparison results

Radiation quality	6 MV	10 MV	18 MV
$N_{D_w,\mathrm{KRISS}} \big/ N_{D_w,\mathrm{BIPM}}$ using sn 8979	1.0081	1.0056	1.0085
$N_{D_w,\mathrm{KRISS}} \big/ N_{D_w,\mathrm{BIPM}}$ using sn 9304	1.0076	1.0056	1.0085
s_{tr}	0.0001		
$\boldsymbol{R_{D\mathrm{w,KRISS}}}$	**1.0078**	**1.0056**	**1.0085**

The results shown in Table 11 demonstrate the agreement between the two standards for absorbed dose to water at the level of 7 parts in 10^3 which is within the relative expanded uncertainty of the comparison of 12 parts in 10^3 evaluated below.

Uncertainties

The uncertainties associated with the BIPM primary standard are listed in Table 12 and those for the transfer chamber calibrations in Table 13. For the KRISS, the uncertainties are listed in Table 14 and Table 15 for the standard and the chamber calibrations, respectively.

The combined standard uncertainty u_{c} for the comparison results $R_{D\mathrm{w,KRISS}}$ is given in Table 16.

Table 12. Uncertainties associated with the BIPM standard

Relative standard uncertainty [(1)]	$u_{i\mathrm{A}}$	$u_{i\mathrm{B}}$
$N_{D\mathrm{c}}$	0.23	0.14
$C_{\mathrm{w,c}}$	0.05	0.25
$k_{\mathrm{rn,BIPM}}$		0.10
Q_{w}	0.10	0.05
k_{vol}		0.03
k_{s}		0.05
depth		0.05
$D_{\mathrm{w,BIPM}}$	0.26	0.32

[(1)] expressed as one standard deviation.

$u_{i\mathrm{A}}$ represents the relative uncertainty estimated by statistical methods, type A

$u_{i\mathrm{B}}$ represents the relative uncertainty estimated by other methods, type B.

Table 13. Uncertainties associated with the calibration of the chambers at the BIPM

Relative standard uncertainty	$u_{i\mathrm{A}}$	$u_{i\mathrm{B}}$
$D_{\mathrm{w,BIPM}}$	0.26	0.32
$Q_{\mathrm{w,transfer}}$	0.02	0.05
depth		0.05
distance		0.02
$k_{\mathrm{rn,transfer}}$		0.05
$k_{\mathrm{s,transfer}}$		0.03
short-term reproducibility	0.07	
monitoring		0.10
$N_{D_{\mathrm{w}},\mathrm{BIPM}}$	0.27	0.35

Table 14. Uncertainties associated with the KRISS standard

Relative standard uncertainty	u_{iA}	u_{iB}
$C_{C,eff}$ effective heat capacity of the core	0.08	0.24
$m_{eff,KRISS}$ effective mass of the core		0.05
$\Delta T_{irr}/Q_{mon}$ temperature rise normalized to the monitor charge	0.03	0.04
k_{BS} different backscattering to the monitor chamber		0.05
(D_W/D_C) conversion factor		0.19
$k_{C,rn,KRISS}$ radial non-uniformity of the beam		0.10
$k_{C,pos}$ radial displacement of the core from the beam centre		0.03
$k_{C,SCD}$ distance difference of the core from reference distance		0.06
$D_{W,KRISS}/Q_{mon}$	0.09	0.34

Table 15. Uncertainties associated with the calibration of the chambers at the KRISS

Relative standard uncertainty	u_{iA}	u_{iB}
$D_{W,KRISS}/Q_{mon}$	0.09	0.34
$Q_{W,KRISS}/Q_{mon}$ charge normalized to the monitor charge	0.01	0.04
k_{elec}, calibration of the electrometer		0.05
k_{TP} temperature and pressure		0.04
k_s ion recombination		0.05
$k_{Q,rn,KRISS}$ radial non-uniformity of the beam		0.15
$k_{Q,pos}$ radial displacement of the chamber from the beam center		0.03
$k_{Q,SCD}$ distance difference of the cavity from reference distance		0.06
$k_{Q,depth}$ difference from reference water depth		0.05
$N_{D_w,KRISS}$	0.09	0.39

Table 16. Uncertainties associated with the comparison result

Relative standard uncertainty	u_{iA}	u_{iB}
$N_{D_w,KRISS}/N_{D_w,BIPM}$	0.28	0.52
Stability s_{st}	0.05	-
Transfer chambers s_{tr}	0.01	-
$R_{D_w,KRISS}$	0.60	

7. Degrees of equivalence

Following a decision of the CCRI, the BIPM determination of the dosimetric quantity, here $D_{w,BIPM}$, is taken as the key comparison reference value (KCRV) (Allisy-Roberts *et al.* 2009, Picard *et al.* 2013). It follows that for each NMI *i* having a BIPM comparison result x_i with combined standard uncertainty u_i, the degree of equivalence with respect to the reference value is the relative difference $D_i = (D_{wi} - D_{w,BIPMi})/ D_{w,BIPMi} = x_i - 1$ and its expanded uncertainty $U_i = 2\ u_i$.

The results for D_i and U_i are expressed in mGy/Gy. Table 17 gives the values for D_i and U_i for each NMI, *i*, taken from the BIPM key comparison database (KCDB 2019) and this report. These data are presented graphically in Figure 4.

Table 17. Degrees of equivalence

Beam quality corresponding to measured $TPR_{20,10}$ between 0.63 (excluded) and 0.71 (included)

Lab *i*	D_i / (mGy / Gy)	U_i / (mGy / Gy)
NRC	-2.7	11.0
PTB	1.3	10.4
NIST	3.5	11.4
LNE-LNHB	-4.8	8.8
ARPANSA	-3.5	11.0
NPL	-2.7	12.4
VSL	-4.1	10.8
NMIJ	-3.4	9.4
NIM	-8.3	12.0
KRISS	7.8	12.0
METAS	-1.7	13.2

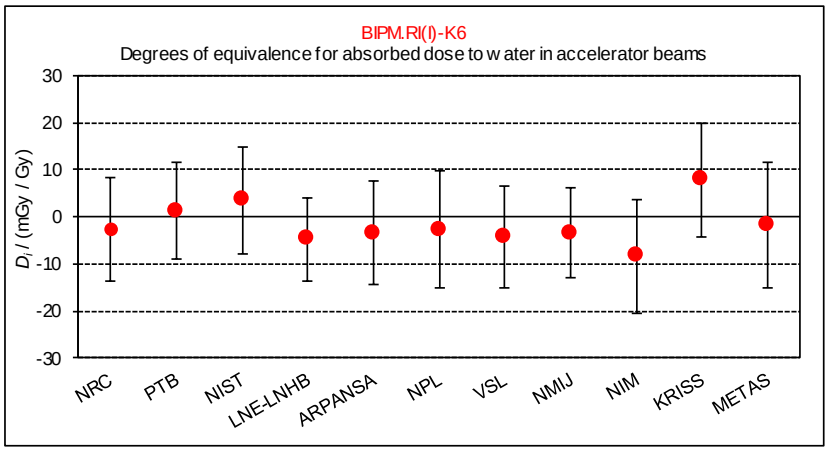

Figure 4. Graph of the degrees of equivalence with the KCRV

Beam quality corresponding to measured $TPR_{20,10}$ between 0.71 (excluded) and 0.77 (included)

Lab *i*	D_i / (mGy / Gy)	U_i / (mGy / Gy)
NRC	0.8	11.0
PTB	3.4	11.4
LNE-LNHB	-5.2	9.4
ARPANSA	-7.6	12.0
NPL	-0.5	13.2
VSL	-4.2	12.8
NMIJ	-4.1	11.0
NIM	-5.9	11.8
KRISS	5.6	12.0
METAS	-3.2	13.2

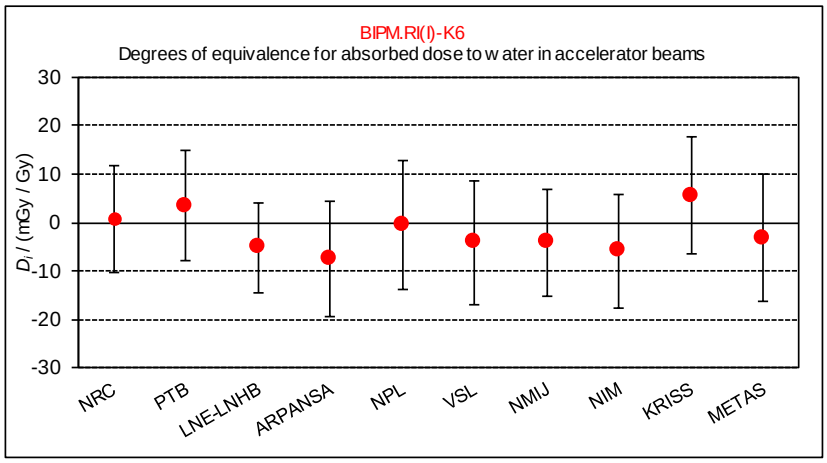

Figure 4. Graph of the degrees of equivalence with the KCRV

Beam quality corresponding to measured $TPR_{20,10}$ between 0.77 (excluded) and 0.81(included)

Lab *i*	D_i / (mGy / Gy)	U_i
NRC	-5.8	11.0
PTB	1.8	12.8
NIST	-4.2	11.8
LNE-LNHB	-6.2	10.0
ARPANSA	-6.8	11.8
NPL	-4.3	16.2
VSL	-0.9	15.0
KRISS	8.5	12.0
METAS	-1.2	13.2

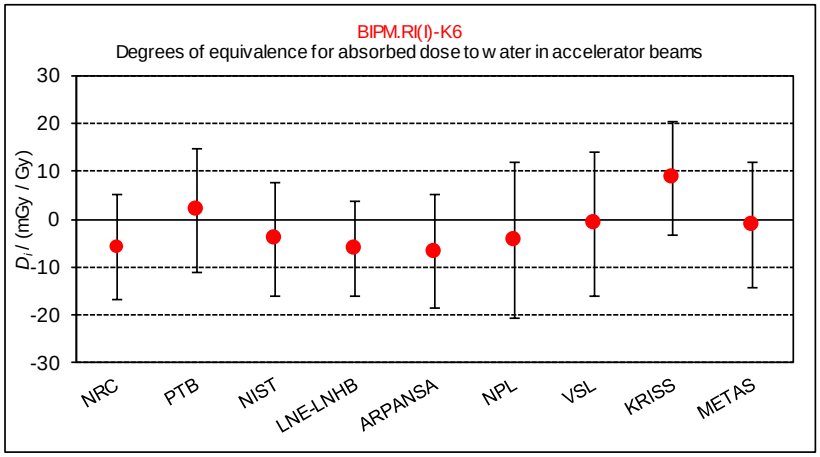

Figure 4. Graph of the degrees of equivalence with the KCRV

8. Conclusions

A key comparison has been carried out between the KRISS and the BIPM standards for absorbed dose to water in accelerator photon beams, using two ionization chambers as transfer instruments. The comparison result is evaluated as the ratio of the calibration coefficients measured by the KRISS and the BIPM. The results show the standards to be in agreement within the expanded standard uncertainty of the comparison of 12 parts in 10^3.

Note that the data presented in the tables, while correct at the time of publication of the present report, become out of date as laboratories make new comparisons with the BIPM. The formal results under the CIPM MRA are those available in the BIPM key comparison database (KCDB 2019).

References

Allisy P J, Burns D T and Andreo P 2009 International framework of traceability for radiation dosimetry quantities *Metrologia* **46(2)** S1-S8

Boutillon M 1998 Volume recombination parameter in ionization chambers *Phys. Med. Biol.,* **43**, 2061-2072

Burns D T 2019 The dose conversion procedure for the BIPM graphite calorimeter standard for absorbed dose to water, in preparation

Burns D T and McEwen M R 1998 Ion recombination corrections for the NACP parallel-plate chamber in a pulsed electron beam *Phys. Med. Biol.,* **43**, 2033-2045

International Atomic Energy Agency 2000 Absorbed Dose Determination in External Beam Radiotherapy. An International Code of Practice for Dosimetry Based in Standards of Absorbed Dose to Water *Technical Report Series* No 398 (IAEA Vienna)

Kawrakow I, Mainegra-Hing E, Rogers D W O, Tessier F, and Walters B R B 2015 The EGSnrc Code System: Monte Carlo simulation of electron and photon transport *Technical Report PIRS-701* (CNRC Canada).

KCDB 2019 BIPM Key Comparison Database Measurement of absorbed dose to water for high-energy photon beams BIPM.RI(I)-K6

Kim I J, Kim B C, Kim J H, Chung J P, Kim H M and Yi C –Y 2017 Building a Graphite Calorimetry System for the Dosimetry of Therapeutic X-ray Beams *Nucl. Eng. Technol.*, **49**, 810-816

Ostrowsky A and Daures J 2008 The Construction of the Graphite Calorimeter GR9 at LNE-LNHB (Geometrical and Technical Considerations) *Rapport* CEA-R-6184 (Saclay: LNHB)

Picard S, Burns D T and Roger P 2009 Construction of an Absorbed-Dose Graphite Calorimeter *Rapport* BIPM-2009/01 (Sèvres: Bureau International des Poids et Mesures)

Picard S, Burns D T and Ostrowsky A 2011 Determination of the recombination correction for the BIPM parallel-plate ionization chamber type in a pulsed photon beam *Rapport* BIPM-2011/06 (Sèvres: Bureau International des Poids et Mesures)

Picard S, Burns D T and Los Arcos J M 2013 Establishment of degrees of equivalence of national primary standards for absorbed dose to water in accelerator photon beams *Metrologia* **50** *Tech. Suppl.* 06016

Picard S, Kessler C, Roger P and Burns D T 2016 Key comparison BIPM.RI(I)-K6 for the standards of absorbed dose to water at 10 g cm^{-2} of the NIM, China and the BIPM in accelerator photon beams *Metrologia* **54** *Tech. Suppl.* 06009

Salvat F, Fernandez-Varea J M and Sempau J 2011 PENELOPE-2011: A Code System for Monte Carlo Simulation of Electron and Photon Transport *NEA/NSC/DOC(2011)5 Workshop Proc. (Barcelona, Spain 4 – 7 July 2011)* (Paris: OECD NEA)

Seuntjens J P and DuSautoy A R 2003, Review of calorimeter based absorbed dose to water standards, in: *Proceedings of International Symposium on Standards and Codes of Practice in Medical Radiation (Vienna, Nov. 2002) IAEA-CN-96-3* **Vol. 1** 37-66